JOURNAL OF GEOPHYSICAL RESEARCH, VOL. 115, B07406, doi:10.1029/2009JB007022, 2010

Volcano monitoring using GPS: Developing data analysis strategies based on the June 2007 Kīlauea Volcano intrusion and eruption

Kristine M. Larson,[1] Michael Poland,[2] and Asta Miklius[2]

Received 1 October 2009; revised 8 January 2010; accepted 15 January 2010; published 13 July 2010.

[1] The global positioning system (GPS) is one of the most common techniques, and the current state of the art, used to monitor volcano deformation. In addition to slow (several centimeters per year) displacement rates, GPS can be used to study eruptions and intrusions that result in much larger (tens of centimeters over hours-days) displacements. It is challenging to resolve precise positions using GPS at subdaily time intervals because of error sources such as multipath and atmospheric refraction. In this paper, the impact of errors due to multipath and atmospheric refraction at subdaily periods is examined using data from the GPS network on Kīlauea Volcano, Hawai'i. Methods for filtering position estimates to enhance precision are both simulated and tested on data collected during the June 2007 intrusion and eruption. Comparisons with tiltmeter records show that GPS instruments can precisely recover the timing of the activity.

Citation: Larson, K. M., M. Poland, and A. Miklius (2010), Volcano monitoring using GPS: Developing data analysis strategies based on the June 2007 Kīlauea Volcano intrusion and eruption, *J. Geophys. Res.*, *115*, B07406, doi:10.1029/2009JB007022.

1. Introduction

[2] The study of volcanoes continues to benefit from the revolution in space geodesy (see e.g., *Dzurisin* [2007]). Space-based techniques such as interferometric synthetic aperture radar (InSAR) provide high-spatial-density images of volcano deformation, often in regions that are difficult to instrument on the ground [*Jónsson et al.*, 1999; *Pritchard and Simons*, 2004]. In contrast, global positioning system (GPS) volcano monitoring systems must be installed on the ground and thus are at risk of destruction during eruptions and may be influenced by adverse weather conditions or other problems [*Cervelli et al.*, 2006; *Lisowski et al.*, 2008]. Nevertheless, a GPS monitoring system has the advantage that it can place precise constraints on the timing of eruptions that cannot be retrieved from InSAR data. It also provides three-dimensional positions that complement terrestrial deformation data sets that are sensitive at other timescales (i.e., continuous tilt and strain).

[3] GPS receivers routinely collect data at fairly high sampling rates (15 or 30 s), but it is less common to estimate positions at those rates. Most GPS studies of deformation on volcanoes are based on 24-h averaged positions [*Cervelli et al.*, 2002a, 2002b, 2006; *Lisowski et al.*, 2008]. This is clearly advantageous when deformation rates are relatively slow, <5 mm/d. In addition to daily positions, *Owen et al.* [2000] and *Segall et al.* [2001] used hourly GPS solutions to examine large signals associated with a dike intrusion. *Irwan et al.* [2003] estimated 30 s GPS positions in their study of Miyakejima volcanic event of June 2000. No evaluation of coordinate precision is given by *Irwan et al.* [2003], but it is clear that the noise level is small compared to the very large signals for this event, 40 cm subsidence and 80 cm lengthening.

[4] Recent work that demonstrated GPS positions estimated at 1 s could be used to observe seismic displacements [*Larson et al.*, 2003; *Bock et al.*, 2004; *Ji et al.*, 2004] suggests that volcano monitoring should also move to sampling (and positioning) rates of 1 s, particularly since existing GPS receivers can be operated at 1 or 30 s at the same cost (telemetry for the two data streams is a separate issue). Some initial work at these higher sampling rates has already been done. For example, *Mattia et al.* [2004] collected GPS data on Stromboli Island at 1 s but then averaged positions for 10 min time periods. Presumably 10 min was chosen to reduce noise in the average position estimates, but the trade-off between precision and averaging interval is not known. The methodology used by *Mattia et al.* [2004] is well suited to real-time monitoring but is limited to short baselines (several km), reporting 5 and 25 mm precision in the horizontal and vertical coordinates, respectively. *Patanè et al.* [2007] also calculated 1 s GPS positions for the Stromboli volcano but passband filtered the data at 2–5 min periods to study the magmatic system.

[5] This paper is an update of a previous assessment of GPS data analysis strategies for volcano monitoring [*Larson et al.*, 2001]. In that work, data from the GPS network on Kīlauea Volcano were used to evaluate Kalman filtering strategies in an effort to optimize subdaily position estimates. Only position results at 15 min time intervals were

[1]Department of Aerospace Engineering Sciences, University of Colorado, Boulder, Colorado, USA.
[2]U.S.G.S. Hawaiian Volcano Observatory, Hawai'i Volcanoes National Park, Hawai'i National Park, Hawai'i, USA.

0148-0227/10/2009JB007022

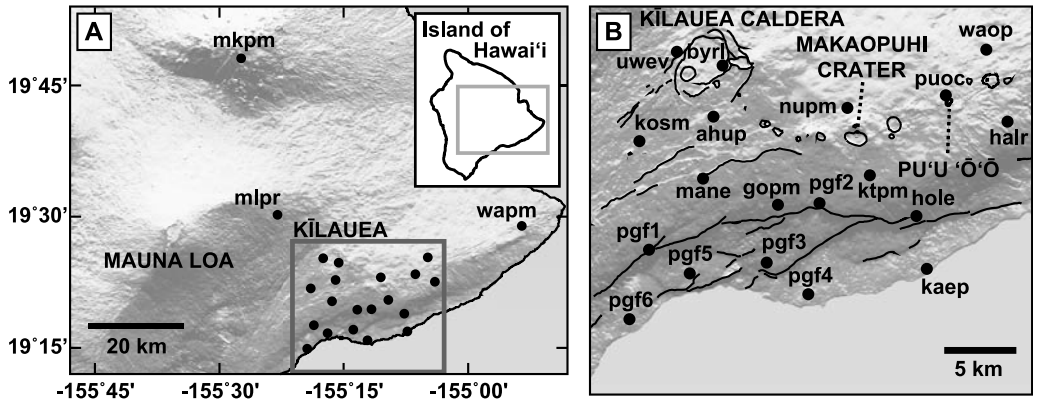

Figure 1. (a) Location of GPS sites used in this study; (b) a more detailed map of the area outlined in (a) showing GPS sites on Kīlauea used in this study.

discussed. The geophysical signals used to test the Kalman filtering methods were quite small, with a maximum size of 3 cm. The data used in that study were collected in the first half of 1998. This study focuses on a data set collected nearly 10 years later, in June 2007. In the decade between the two studies, there have been numerous changes in the GPS system. The GPS constellation is now ~15% larger. International Terrestrial Reference Frame 2005 (ITRF2005), a newer and more accurate terrestrial reference frame [*Altamimi et al.*, 2007], is embedded in the International Global Navigation Satellite Systems Service (IGS) [*Beutler et al.*, 1994] orbits used in data processing. The IGS orbits currently report an average radial RMS precision of 8 mm, whereas in 1998 the stated precision of orbits computed in the ITRF94 reference frame was 32 mm. Improved orbit precisions directly relate to improved positioning precision. Another important improvement in the last decade has been the availability of more precise troposphere modeling strategies [e.g., *Bar-Sever et al.*, 1998]. All of these changes should produce better precision in GPS position estimates at higher sampling rates than was possible a decade ago. We also have the opportunity to test high-rate GPS data analysis strategies on a larger geophysical signal than was available to *Larson et al.* [2001] (i.e., the June 2007 Kīlauea Volcano dike intrusion and eruption) [*Poland et al.*, 2008; *Montgomery-Brown et al.*, 2010].

2. Geologic Setting

[6] Since 1983, Kīlauea Volcano, on the island of Hawai'i, has erupted almost continuously from the Pu'u 'Ō'ō and Kupaianaha vents on the east rift zone (Figure 1) [*Heliker and Mattox*, 2003]. These vents are fed by magma that is transported laterally from storage reservoirs beneath the volcano's summit caldera [e.g., *Cervelli and Miklius*, 2003]. The Pu'u 'Ō'ō-Kupaianaha eruption has been interrupted on several occasions by small intrusions and eruptions between the summit and Pu'u 'Ō'ō. These events result in rapid summit deflation and collapse of the Pu'u 'Ō'ō cone (as magma drains from both areas to feed the intrusion or eruption) and in dilation of the rift zone due to magma injection, as exemplified by events in 1997 [*Owen et al.*, 2000] and 1999 [*Cervelli et al.*, 2002a].

[7] The most geodetically well characterized of these east rift zone intrusions and eruptions occurred in 2007. At 12:16 Coordinated Universal Time (UTC) on 17 June (the Father's Day holiday), rapid summit deflation began coincident with the onset of a seismic swarm and dilation at the east rift zone. Sometime during the local night of 18 and 19 June, a small eruption occurred on the east rift zone between the summit and Pu'u 'Ō'ō. Summit deformation switched to inflation at 20:30 UTC on June 19, indicating the end of the Father's Day intrusion/eruption. During this event the summit caldera subsided by a maximum of ~0.12 m near Halema'uma'u Crater, while the east rift zone dilated by a maximum of about 1 m near Makaopuhi Crater. The reader is directed to *Poland et al.* [2008] and *Montgomery-Brown et al.* [2010] for additional information on the Father's Day event.

[8] Although most GPS sites on Kīlauea were dominated by signals associated with the intrusion during 17–19 June, GPS sites on the coast, far from the summit and east rift zone and outside the region affected by intrusion-related deformation, experienced displacements consistent with aseismic flank slip. This deformation started about 15–20 h after the initiation of the intrusion, leading *Brooks et al.* [2008] to hypothesize that the Father's Day intrusive/eruptive activity triggered a slow earthquake.

[9] At the time of the Father's Day eruption and intrusion, there were 20 GPS stations operating on Kīlauea Volcano (Figure 1). The default sampling interval for all GPS receivers was 30 s, although some receivers recorded data at 1 s. Most of the stations have antennas on masts in concrete pillars or metal monuments about 1 m high, cemented into bare or ash-mantled lava flows. The sites UWEV, AHUP, and BYRL are most sensitive to motions near Kīlauea caldera, while the middle-east rift zone is monitored by two rift-crossing baselines (NUPM-KTPM and HALR-WAOP). One GPS station was located on Pu'u 'Ō'ō (PUOC), and several stations measure deformation of Kīlauea's mobile south flank (PGF1-6, GOPM, MANE, KAEP, and HOLE). One station tracks deformation in the southwest rift zone (KOSM) and one station monitors the lower-east rift zone (WAPM). This study focuses on data recorded at the summit, south flank, and middle-east rift zone. Modeling of the GPS data is discussed

by *Montgomery-Brown et al.* [2010]; this paper emphasizes resolution of the GPS data.

3. Subdaily GPS Data Analysis Methodologies

[10] Any GPS data analysis strategy should be based on a careful evaluation of both the frequency band of the geophysical signal of interest and likely GPS error sources. Overall, subdaily GPS position estimates are affected by the same error sources as daily averaged positions. But with GPS (radial) orbit precisions of better than 1 cm, the most important error sources impacting subdaily GPS precision are multipath and water vapor. We also will also discuss the impact of receiver sampling rate, averaging and filtering on positioning precision. We discuss these issues in turn.

3.1. Multipath

[11] There are no physics-based multipath models used in routine analysis of GPS data. There are, however, empirically based multipath models which for some situations are very helpful. For example, modified sidereal filtering [*Genrich and Bock*, 1992; *Choi et al.*, 2004] or aspect repeat time adjustment [*Larson et al.*, 2007] has been shown to reduce multipath error in 1 s GPS data sets. It has been less rigorously tested for the 30 s data typically available in the Hawai'i data set. Nevertheless, if the multipath periods are sufficiently long (for reflections from the ground, multipath periods depend on antenna height), a technique like modified sidereal filtering should reduce multipath errors. Ground multipath for antenna heights in the range 0.5–2 m used in Hawaii produces errors at periods of ~30–10 min, meaning that the 30 s sampled data should be more than adequate for modeling multipath, if the ground surface at Kīlauea GPS sites produces strong specular (mirror-like) reflections.

[12] Evidence of ground multipath (or lack thereof) can be seen in the signal-to-noise ratio (SNR) data or in the power spectra of high-rate positions. *Bilich and Larson* [2007] advocated making frequency-specific multipath maps, but their code (1) was never generalized for common usage and (2) did not specifically address ground multipath frequencies. Here we show that a simple examination of the raw SNR data can be used to evaluate whether ground reflections are prevalent in the data. Since multipath signals are much stronger at low elevation angles, this analysis only includes measurements between 10° and 25° elevation angles.

[13] Figure 2 shows SNR data for 12 Kīlauea GPS sites (PGF1-3 and PGF6 are Ashtech Z-12 s, the remainder are Trimbles NetRSs), 1 GPS site in southern California (DHLG, Ashtech Z-12), and another from Colorado (P041, Trimble NetRS), and a simulation. For the latter, we use the analytic results for a planar horizontal reflector described by *Georgiadou and Kleusberg* [1988] and extended by *Larson et al.* [2008]. DHLG and P041 were chosen as comparison sites because (1) they use the same receivers as the Kīlauea network and (2) their (specular) multipath characteristics have previously been evaluated [*Larson et al.*, 2007, 2008]. In other words, we know that multipath modeling works at these sites. Both choke rings and zephyr antenna types are used in Kilauea. While both antenna types mitigate multipath effects, neither remove them entirely. Because SNR data are fairly noisy, tracks for multiple satellites in one quadrant are shown and averaged. In this example, the southeast azimuths were used.

[14] Because multipath periods are not intuitively obvious, we have also simulated L1 SNR data for a perfect reflector at the two antenna heights most common used at Kīlauea (2.0 and 0.7 m). DHLG and P041 show very clear constant frequency oscillations that are consistent with their ~1.8 m antenna heights and theory. The simulations agree reasonably well with the SNR observations at only two HVO sites: BYRL and PGF6, with slight correlation at KAEP. There is no correlation at the other HVO sites. Figure 2 underscores the site-specific character of multipath and serves as a cautionary tale. Even if multipath modeling works in one region [*Langbein and Bock*, 2004; *Choi et al.*, 2004; *Larson et al.*, 2007], as was shown for sites in California, it does not mean that it can be modeled successfully in your network. The failure of multipath models for some of the stations in the Kīlauea data set is likely related to the nonuniformity of the reflecting surface (generally barren or ash-mantled pahoehoe lava), where ridges, troughs, and surface blocks are tilted in dimensions that are close to the GPS wavelengths (19 and 24.4 cm).

3.2. Atmospheric Water Vapor

[15] For the past two decades, the geodetic community has continually adapted its troposphere modeling strategies to improve positioning precision. Part of the improvement has come from developments in mapping functions [*Niell*, 1996; *Boehm et al.*, 2006] and tracking satellites to lower elevation angles. The introduction of azimuthal troposphere gradient terms [*Bar-Sever et al.*, 1998] has also enhanced positioning precision [*Miyazaki et al.*, 2003]. However, there is little literature on how to utilize gradients when significant time-varying displacements occur. Another issue relates to the gradients themselves. Default analysis strategies frequently use a constant gradient for a 24-h period. *Mattia et al.* [2004] and *Larson et al.* [2007] did not use gradients at all when evaluating GPS analysis methods for 1 s positioning. The GIPSY software used in this study treats gradients as a stochastic parameter, and thus allowing time-varying behavior is straightforward. But it would be unrealistic to expect that time-varying position changes and time-varying gradients could be estimated simultaneously without some degradation of positioning precision.

[16] The first question we can address is as follows: How variable are azimuthal troposphere gradients in the Kīlauea network? This might at least demonstrate the validity of using no gradients or a single 24 h gradient. Previous studies using GPS data from the island of Hawai'i suggest that zenith delays in the GPS signal due to the water content of the troposphere can vary over both time and space [*Foster et al.*, 2003; *Foster and Bevis*, 2003]; thus, there is reason to believe that subdaily azimuthal troposphere gradients will be necessary to improve positioning precision. We used the precise point positioning strategy and products from the Jet Propulsion Laboratory [*Zumberge et al.*, 1997] to compute solutions for 21 and 22 June. Displacements associated with the dike intrusion (which initiated on 17 June) are subcentimeter on these days. The direction and size of the gradient terms are plotted in Figure 3. Colors are used to show time dependence of the gradients. For comparison, we also show gradients estimated for the same days for eight

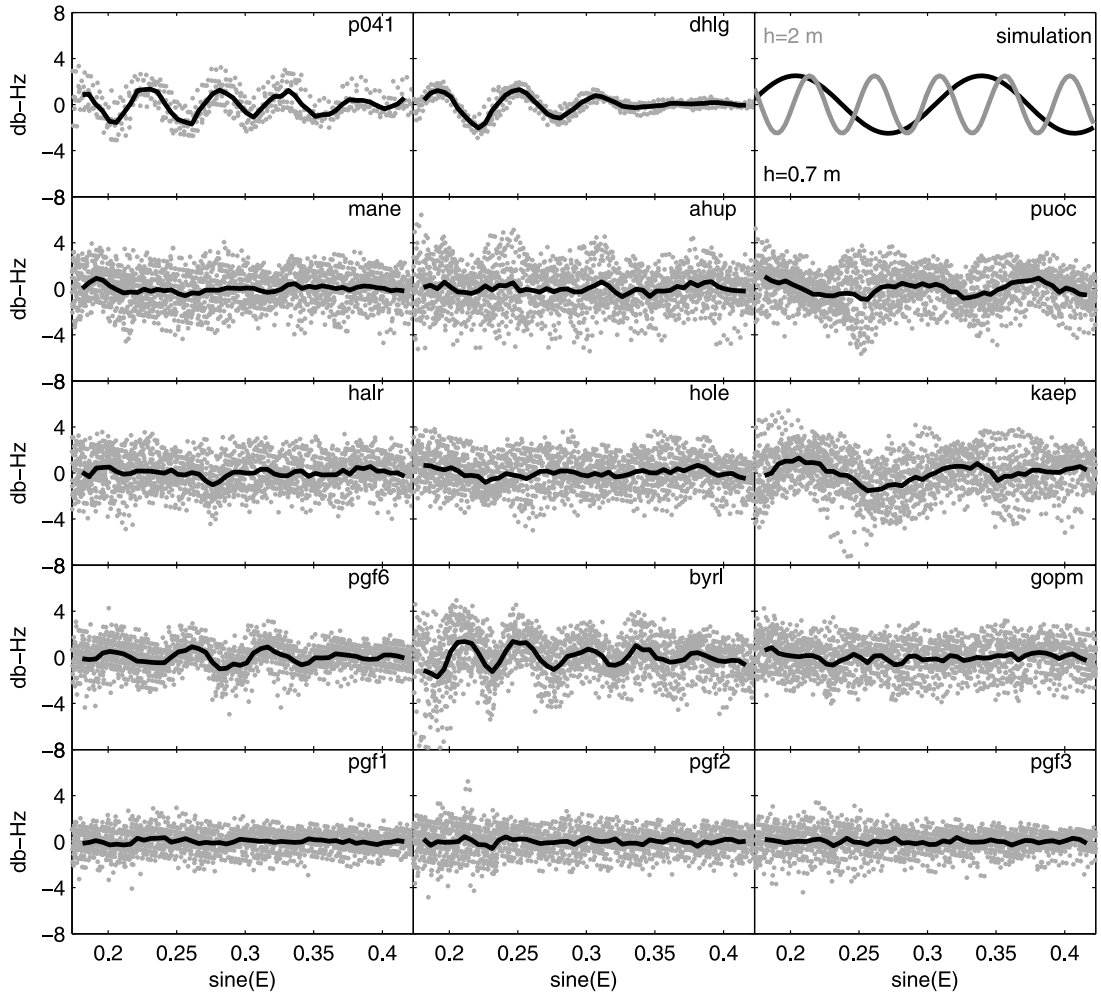

Figure 2. Detrended L1 SNR data for 12 GPS sites from Kīlauea. For comparison, two sites located over bare soil (P041 and DHLG from Colorado and California, respectively) are shown. In the top right corner, simulated SNR data are shown for a station at Kīlauea's latitude/longitude and antenna heights of 0.7 and 2.0 m. Since the ground is modeled as a horizontal, planar reflector, the multipath oscillations have a constant frequency as a function of sine of the satellite elevation angle. All plots are restricted to elevation angles between 10° and 25°.

sites in the Parkfield GPS array. These sites have been used extensively for high-rate GPS studies [*Langbein and Bock*, 2004; *Langbein et al.*, 2006; *Choi et al.*, 2004]. Note that, overall, the Parkfield gradient terms are much smaller and vary little with time. This explains why estimating a constant tropospheric gradient term for a 24 h period might be appropriate for Parkfield but not on Kīlauea. Not estimating a gradient might also work at Parkfield when assessing differential positions, because most of the error would be present in both solutions. The situation at Kīlauea is quite different. The gradients on 21 and 22 June bear little resemblance to each other although the stations are only 5–20 km apart. Furthermore, the gradients are 2–3 times larger than those observed at Parkfield. We will be unable to estimate accurate subdaily positions at Kīlauea if this variation in tropospheric delay is not properly modelled.

3.3. Sampling, Averaging, and Filtering

[17] The vast majority of Kīlauea GPS receivers record measurements every 30 s, and intrinsically this limits how often positions can be estimated. The secondary questions are (1) how often should positions be estimated and (2) should the positions be filtered. The first question is clearly determined by the geophysical signal of interest. If a geophysical signal is tens of millmeters per second, as it could be for seismic displacements, unconstrained (white noise) positions should be estimated at the highest possible rate. If, however, positions change slowly (e.g., 2–20 mm/h), which is the case for the Father's Day eruption/intrusion, it is better to perform some kind of averaging and produce more accurate positions less frequently. While the next section will refocus this discussion using results from the Father's Day event, here we can review the differences between some end-member estimation strategies.

[18] For this discussion, we will take advantage of the GIPSY software simulation capabilities. While this does not allow us to evaluate the impact of systematic errors, such as multipath and troposphere mismodeling, it does provide guidance on averaging and filtering. White noise position estimates using simulated 30 s data are shown in Figure 4. A

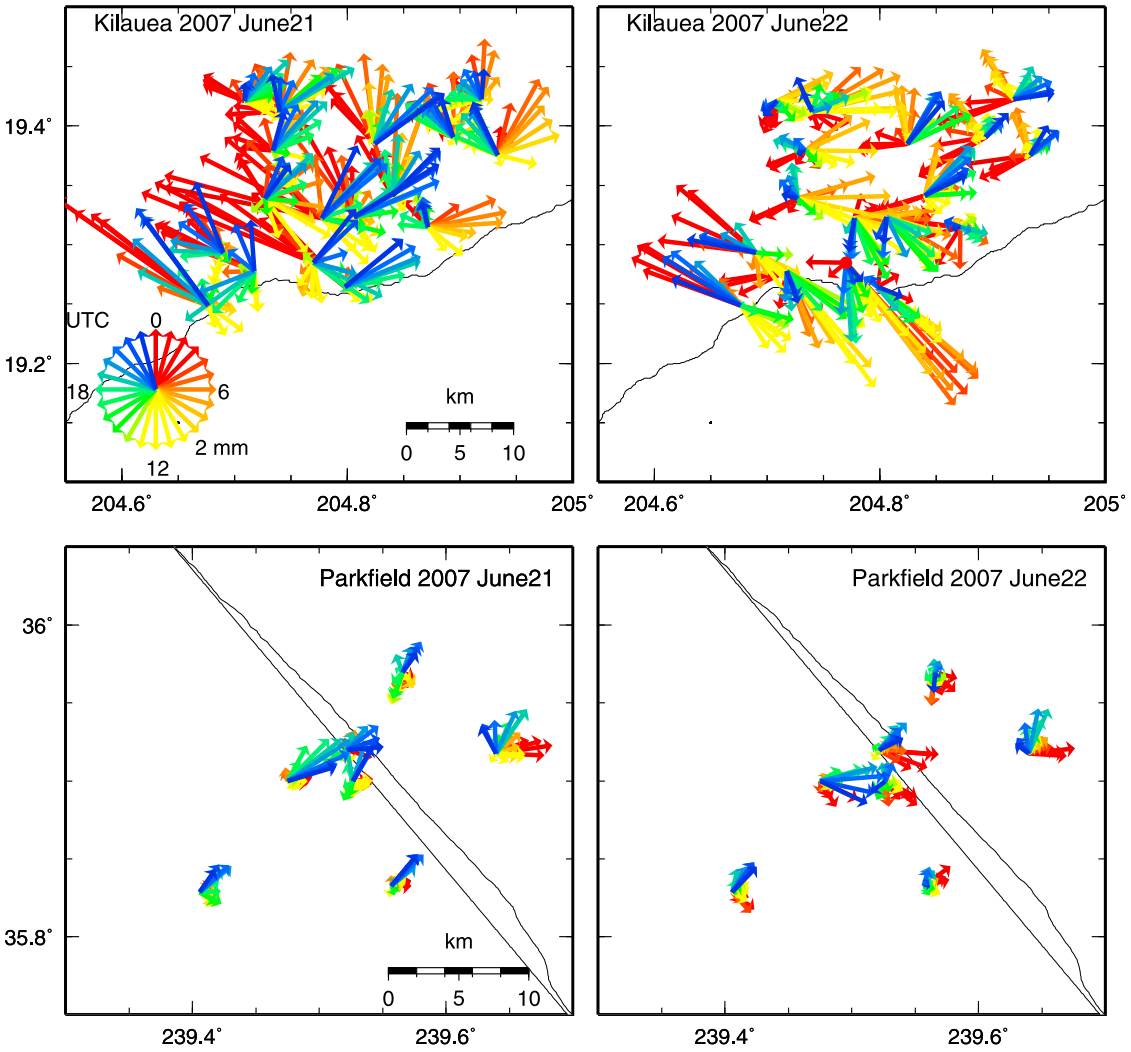

Figure 3. Estimated azimuthal troposphere gradient terms on 21 and 22 June for the Kīlauea and Parkfield GPS networks. Scale (2 mm) is shown. Timing (in UTC) is given by the color scale in the lowerleft corner.

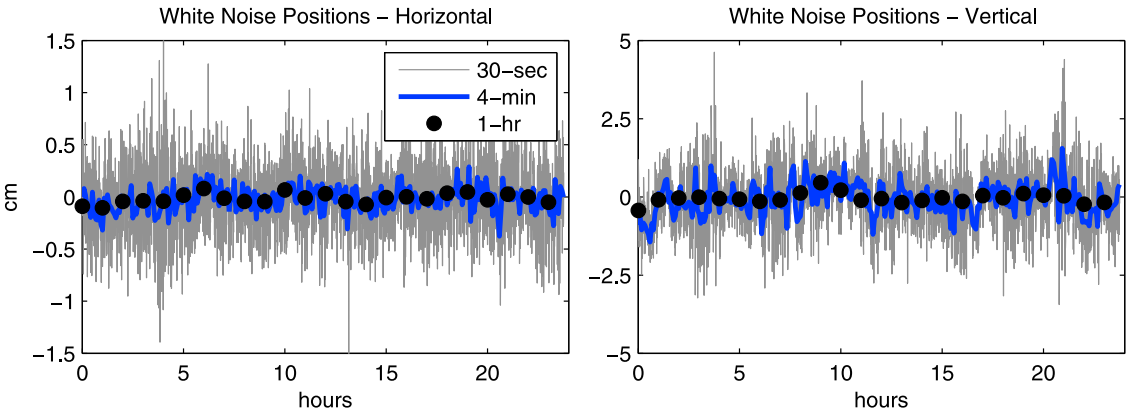

Figure 4. Position simulation for 30-s, 4-min, and 1-h increments using 30-s observations and white noise estimation strategy. Horizontal (left) and vertical (right) components are shown. Note change in scale between horizontal and vertical results.

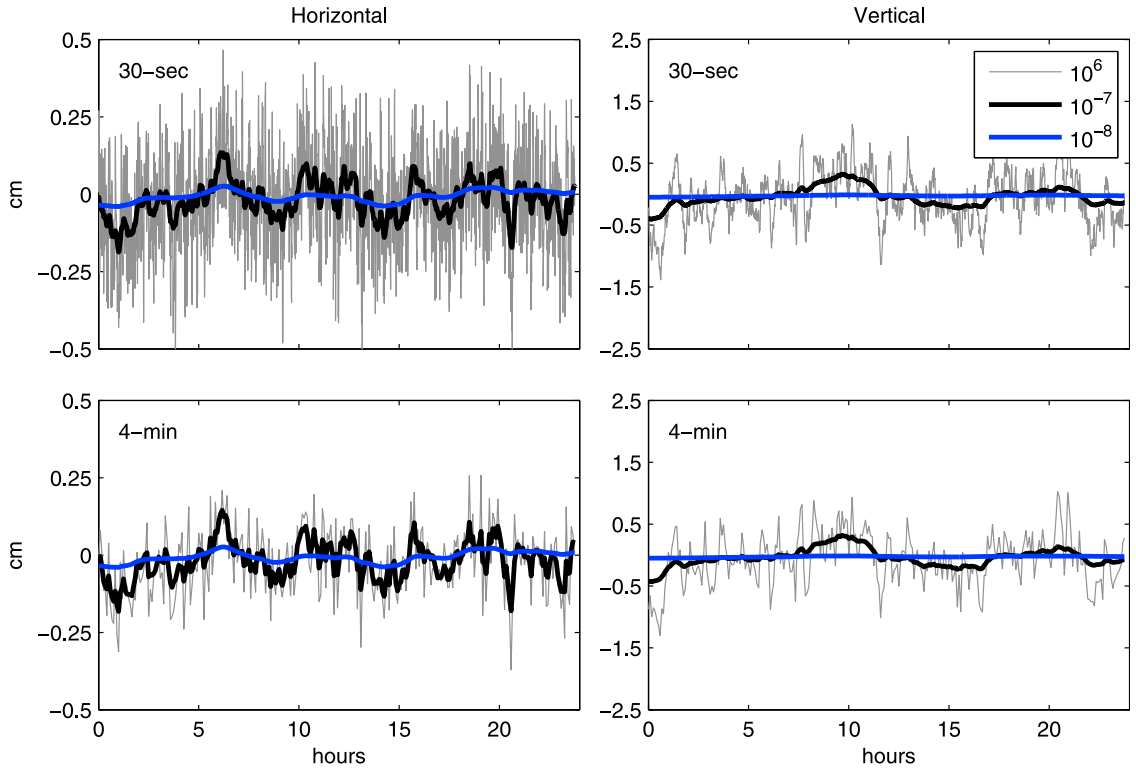

Figure 5. Position simulation for 30-s and 4-min increments using random walk estimation strategy. The value of σ_{rw} used is given in units of km/$\sqrt{s}$. Horizontal and vertical components are shown in the left and right columns, respectively.

carrier phase noise level of 5 mm was assumed. The same orbits that will be used to analyze data from the Father's Day event were used for the simulation. A site on Kīlauea (AHUP) and the same time epoch (15 June 2007) was used to ensure that the same satellite geometry is used as was available during the dike intrusion. Three estimation intervals are compared: 30 s, 4 min, and 1 h. In both horizontal and vertical components, the 30 s positions show the largest random variations. These are significantly reduced by averaging measurements into 4 min positions, yielding standard deviations of 1.4 mm horizontally and 4.9 mm vertically. Finally, hourly positions are also shown. For very small geophysical signals (millimters per day), these hourly measurements would clearly be sufficient and preferred.

[19] Beyond white noise positions, we can impose smoothing using a Kalman filter random walk parameterization. As discussed in detail by *Elósegui et al.* [1996], the random walk smoothing constraint (σ_{rw}) one chooses depends on how big the signal is and how frequently positions are estimated. Choosing a σ_{rw} that is too small will bias the signal; choosing one that is too large will reduce your ability to resolve the signal because the estimates will be too noisy. Figure 5 displays simulations for multiple values of σ_{rw} using either 30 s or 4 min position estimates. The tightest constraint ($\sigma_{rw} = 10^{-8}$ km/$\sqrt{s}$) yields results that are closest to the truth (which is zero in this case). This simulation also demonstrates that there is no gain in estimating positions every 30 s if strong smoothing is applied, as the results are similar for σ_{rw} of 10^{-8} and 10^{-7} km/$\sqrt{s}$.

4. Results

4.1. Data

[20] GPS data collected between 14–22 June 2007 were analyzed with the GIPSY software [*Lichten and Border*, 1987]. These dates were chosen to encompass the Father's Day intrusion and eruption (17–19 June), with the additional data providing information on the precision of the position estimates. In principle, one could analyze the data for all Kīlauea stations for the 9-day period of this study in one batch. In practice, the GIPSY software has limitations on the number of observations that can be analyzed simultaneously. Because of this, the data were analyzed in subnetworks consisting of 10 stations each for a period of 3 days. Four of these 3 d solutions were analyzed, with a 24 h overlap period to ensure that there were no day-boundary discontinuities. All the 30 s GPS data were used in this analysis, but a position was estimated only every 4 min. This temporal resolution was sufficient for the needs of modeling the event [*Montgomery-Brown et al.*, 2010]. Satellite and receiver clocks were estimated as a white noise process, and the ionosphere-free data combination was used [*Lichten and Border*, 1987]. Precise IGS ephemerides and Earth orientation were held fixed [*Beutler et al.*, 1994]. An elevation angle cutoff of 10° was used. A time-varying zenith tropo-

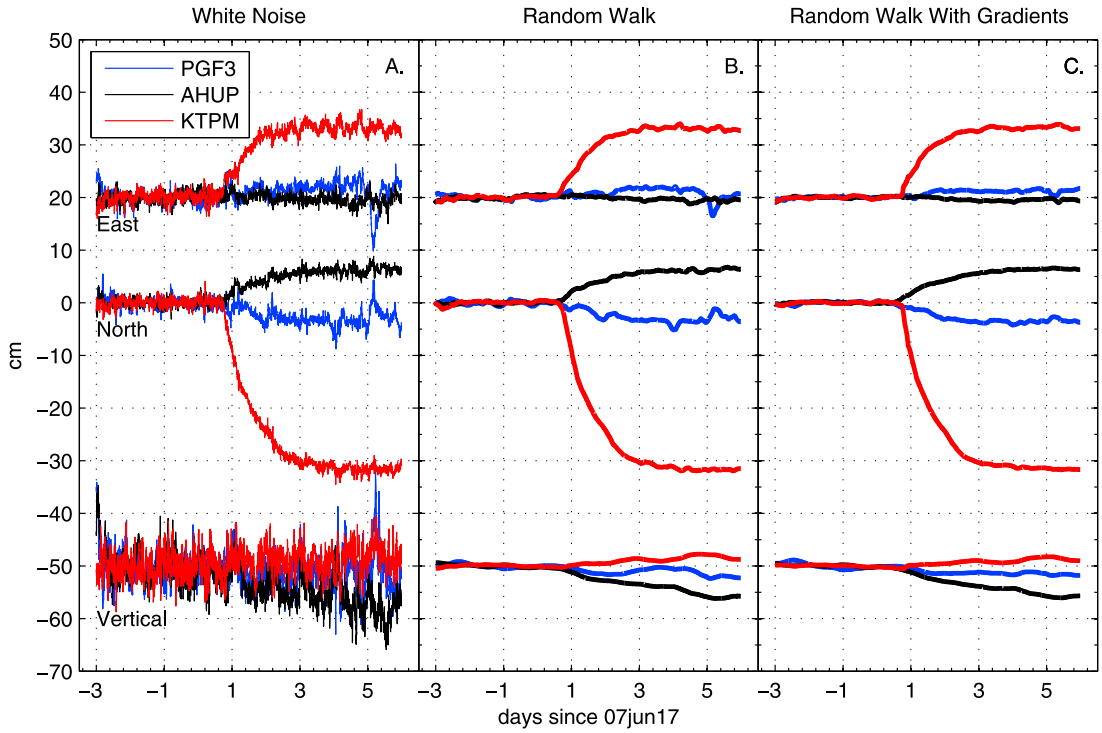

Figure 6. East, north, and vertical time series for PGF3, AHUP, and KTPM. Estimation strategies are (a) white noise position estimation, (b) tight random walk position estimation (σ_{rw} = 10^{-8} km/$\sqrt{s}$), (c) tight random walk position estimation with time-varying troposphere gradients.

sphere delay was estimated with a constraint of 10^{-7} km/$\sqrt{s}$. When estimated, we used a constraint of 5×10^{-9} km/$\sqrt{s}$ for the azimuthal atmospheric gradients [*Bar-Sever et al.*, 1998]. We also constrained the coordinates of three sites far from the deforming zone (MLPR, WAPM, and MKPM, Figure 1a) to their ITRF2005 values; these sites serve as a "minifiducial network" [*Larson et al.*, 1991]. Ambiguity resolution was successful on ~90% of baselines [*Blewitt*, 1989].

4.2. Systematic Errors

[21] Figures 4 and 5 show the kind of positioning precision that can be achieved with GPS when models are perfect and errors in the data are randomly distributed. The geophysical signal in those simulations was the absence of any motion. The Kīlauea data set (examples shown in Figure 6), on the other hand, has both imperfect models and systematic errors. There are also a variety of signals: very large signals (KTPM, >30 cm), substantial deflation at the caldera (AHUP, ~7 cm), and much more subtle signals on the southwest flank (PGF3, <1 cm). Systematic errors are also evident in Figure 6. Assuming that ground motions are fairly smooth after the first day of deformation, significant noise is visible at PGF3 4 days after the event began (June 21). More than 10 cm of east component ground motion occurs in 3 h. There is no volcanic or tectonic signal that can explain the motion at PGF3. Similar excursions are seen at other sites, most notably GOPM (not shown). We can see the signature of this signal more clearly when we apply the tight random walk constraint (σ_{rw} = 10^{-8} km/$\sqrt{s}$). Constraining the motion reduces the apparent signal from 10 to 4 cm.

[22] The apparent PGF3 motion is correlated in time with the large azimuthal troposphere gradients shown in Figure 3. When we reanalyzed the GPS data using both the tight random walk positioning constraint and azimuthal troposphere gradients, there is significant reduction in the position changes at PGF3 on both 21 and 22 June. Adding troposphere gradients also improves positions at longer periods. Figure 7 summarizes the improvement in precision for the entire network when azimuthal troposphere gradients

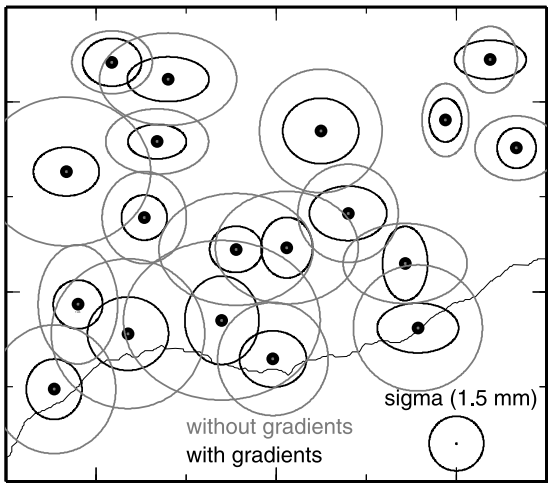

Figure 7. The rms standard deviations for variations in 4-min east and north estimated components (black) with and (gray) without estimated azimuthal troposphere gradients only days before and after the dike intrusion are used to calculate rms. The same value for σ_{rw} was used for each case. Area covered is the same as in Figure 1b.

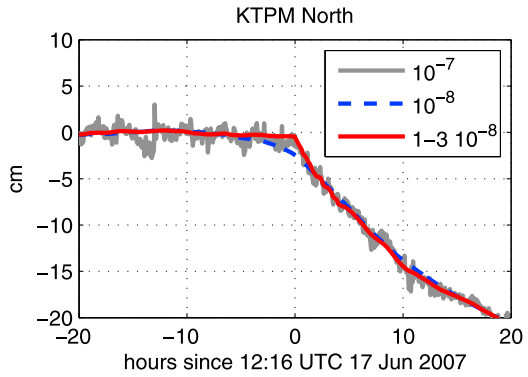

Figure 8. Time series for KTPM for three estimation strategies; σ_{rw} is given in the legend, with units of km/$\sqrt{s}$.

are used. Because of the large displacements during the dike intrusion, only data from 14–16, 21, and 22 June were used to calculate coordinate precisions from the 4 min time series. Sites near the coast (PFG3, GOPM, KAEP) and KOSM show the greatest improvement in precision when gradients are estimated.

4.3. Large Accelerations

[23] Although a tight random walk will reduce the noise in GPS position estimates, as noted by *Elósegui et al.* [1996], overconstraining σ_{rw} will suppress true signals. The sites that clearly show signs of overconstraint with a σ_{rw} of 10^{-8} km/$\sqrt{s}$ are the sites with the largest accelerations, the ERZ crossing sites KTPM and NUPM. In Figure 8 the north component of KTPM is shown. More than 20 cm of motion occurs in 20 h (1 cm/h), but nearly 5 cm of motion is indicated in the first 2 h (2.5 cm/h). Using a parameterization of 10^{-8} km/$\sqrt{s}$ suggests the dike intrusion began nearly 5 h too early. However, if we increase the random walk sigma to 3×10^{-8} km/$\sqrt{s}$ for the first 4 h of the intrusion, we both recover the trend of the loosely constrained solution and the onset of the event. In this example, we did use the a priori knowledge of when the event began to set the σ_{rw} in the filter. In order to recover a much faster deformation rate (25 cm/h), we would have to increase the σ_{rw} by an order of magnitude. We have also found that increasing the σ_{rw} for the caldera sites in the first few hours of the eruption improves the agreement between the constrained random walk and white noise solutions.

5. Discussion

[24] Although we can evaluate the precision of random walk constrained GPS time series in terms of their agreement with simulations, white noise position estimates, and how well they agree with geophysical models [*Montgomery-Brown et al.*, 2010], accuracy can only be determined by comparisons with independent measurements. Of the many geodetic instruments being used on Kīlauea, only tiltmeters have the temporal resolution to provide a useful comparison with GPS. There were 13 tiltmeters operating on Kīlauea during the intrusion, but only one (UWE) is colocated with a GPS receiver (UWEV). The UWE tiltmeter is an Applied Geomechanics model 722 analog tiltmeter. It is installed in a borehole 5 m deep and samples once per minute. Figure 9 shows excellent agreement between the GPS and tilt measurements in the eruption's timing.

[25] What can we learn from the Kīlauea results about monitoring other volcanoes with GPS? One lesson is that geodetic advances in multipath and troposphere modeling may not be necessary (or valid) for your network. The ways we evaluated these error sources are straightforward and easily implemented. For example, SNR data are recorded by all geodetic-quality GPS receivers and do not require significant data processing. And even if your software does not support stochastic troposphere gradients, you can evaluate whether they are needed by free online processing services (http://milhouse.jpl.nasa.gov/ag/). Second, if position changes are slow, as they often are on volcanoes, there is no reason not to incorporate position averaging or Kalman filtering. White noise position estimates can then be used as a check on whether the averaging interval is too long or the Kalman filter constraints are too tight. A final point relates to receiver sampling interval. For most deformation signals on volcanoes, we feel that high-rate (1 s) data are unnecessary. However, the cost of telemetry and archiving 1 s GPS data is becoming cheaper all the time. Maintaining a data stream at this level is not difficult for most users and might be useful for illustrating different signals, such as discussed by *Patanè et al.* [2007]. If signals at seismic frequencies are of interest, then certainly very high-rate GPS data (10 Hz) are not only preferred but also necessary. One way to maintain access to these very high-rate GPS data is to buffer them on the receiver and download them only if needed [*Larson*, 2009].

[26] Finally, what is the relevance of these results to real-time data processing strategies for volcano monitoring? There is really only one difference between what was done here and what needs to be done in real time and this concerns the precision of the orbits. Real-time orbits will always be less precise than postprocessed orbits. Frankly, this is not very limiting for most volcano monitoring because GPS sites on a volcano are likely to be relatively close to each other (e.g., 20–50 km). The effect of orbit errors on baselines of this length (even using real-time orbits) is very small (at the mm level). Rather than intrinsic limitations (such as orbits), the difficulty of real-time GPS volcano monitoring is really one of implementation and

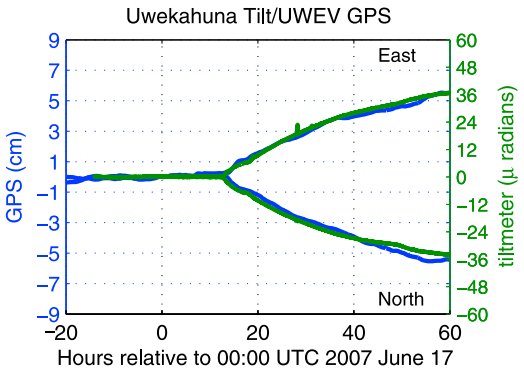

Figure 9. Comparison of GPS and tiltmeter records from the summit caldera. A σ_{rw} of 3 10^{-8} km$\sqrt{s}$ was used in the first 6 h of the event; σ_{rw} of 1 10^{-8} km$\sqrt{s}$ was used before and after the event began.

computational resources. For example, easily the most computationally intensive part of the data analysis described here is ambiguity resolution. This is not because it could not be made faster but more because very fast ambiguity resolution algorithms have been developed and tested for 24 h position solution batches [*Blewitt*, 2008]. They cannot currently be used as configured for either real-time or multiple-day batches. Since subdaily positioning precision significantly benefits from ambiguity resolution, making sure that capability is available for volcano monitoring is strongly encouraged.

6. Conclusions

[27] GPS data from the 2007 Father's Day eruption and intrusion on Kīlauea Volcano have been analyzed to emphasize subdaily resolution of ground motion. The multipath environment and variations in atmospheric water vapor were first evaluated to guide the development of an appropriate data analysis strategy. Based on this analysis, no multipath modeling was attempted. A tightly constrained random walk position estimation strategy was instead used to suppress noise. It was confirmed that time-varying azimuthal troposphere gradients were needed to accurately analyze GPS data from Kīlauea Volcano during this intrusion and eruption. The random walk constraint used was allowed to vary for sites closest to the eruption and intrusion. The resulting GPS time series show good agreement with independent tilt measurements at the Kīlauea summit caldera.

[28] **Acknowledgments.** K.L. would like to acknowledge support from a CU Faculty Fellowship, NSF (EAR0337206 and EAR0538116), and conversations with Mike Lisowski. Reviews from Thora Arnodottir, Dan Dzurisin, John Langbein, and Susan Owen helped us improve the paper. The Kīlauea GPS network is supported by grants from the USGS, NSF, and NASA. The GPS network is operated in collaboration by the USGS, Stanford University (PI: Paul Segall), and Pacific GPS Facility at the University of Hawai'i (PI: Benjamin Brooks). GPS RINEX data are archived at UNAVCO.

References

Altamimi, Z., X. Collilieux, J. Legrand, B. Garayt, and C. Boucher (2007), ITRF2005: A new release of the international terrestrial reference frame based on time series of station positions and Earth orientation parameters, *J. Geophys. Res.*, *112*, B09401, doi:10.1029/2007JB004949.

Bar-Sever, Y., P. Kroger, J. Borjesson (1998), Estimating horizontal gradients of tropospheric path delay with a single GPS receiver, *J. Geophys. Res.*, *103*(B3), 5019–5036, doi:10.1029/97JB03534.

Beutler, G., I. I. Mueller, and R. E. Neilan (1994), The International GPS Service for Geodynamics (IGS): Development and start of official service on January 1, 1994, *Bull. Geod.*, *68*(1), 39–70.

Bilich, A., and K. M. Larson (2007), Mapping the GPS multipath environment using the signal-to-noise ratio (SNR), *Radio Sci.*, *42*, RS6003, doi:10.1029/2007RS003652.

Blewitt, G. (1989), Carrier phase ambiguity resolution for the global positioning system applied to geodetic baselines up to 2000 km, *J. Geophys. Res.*, *94*(B8), 10,187–10,203.

Blewitt, G. (2008), Fixed point theorems of GPS carrier phase ambiguity resolution and their application to massive network processing: Ambizap, *J. Geophys. Res.*, *113*, B12410, doi:10.1029/2008JB005736.

Bock, Y., L. Prawirodirdjo, and T. I. Melbourne (2004), Detection of arbitrarily large dynamic ground motions with a dense high-rate GPS network, *Geophys. Res. Lett.*, *31*, L06604, doi:10.1029/2003GL019150.

Boehm, J., A. Niell, P. Tregoning, and H. Schuh (2006), Global Mapping Function (GMF): A new empirical mapping function based on numerical weather model data, *Geophys. Res. Lett.*, *33*, L07304, doi:10.1029/2005GL025546.

Brooks, B. A., J. Foster, D. Sandwell, C. J. Wolfe, P. Okubo, M. Poland, and D. Myer (2008), Magmatically triggered slow slip at Kilauea volcano, Hawaii, *Science*, *21*(5893), 1177.

Brooks, B. A., J. H. Foster, M. Bevis, L. N. Frazer, C. J. Wolfe, and M. Behn (2006), Periodic slow earthquakes on the flank of Kilauea volcano, Hawaii, *Earth Planet. Sci. Lett.*, *246*(3–4), 207–216.

Cervelli, P. F., and A. Miklius (2003), The shallow magmatic system of Kilauea volcano, in *The Pu'u 'Ō 'ō -Kupaianaha eruption of Kilauea volcano, Hawaii: The First 20 Years*, edited by C. Heliker et al., *U.S. Geol. Surv. Prof. Pap. 1676*, 149–163.

Cervelli, P. F., T. Fournier, J. Freymueller, J. A. Power (2006), Ground deformation associated with the precursory unrest and early phases of the January 2006 eruption of Augustine Volcano, Alaska, *Geophys. Res. Lett.*, *33*, L18304, doi:10.1029/2006GL027219.

Cervelli, P., P. Segall, F. Amelung, H. Garbeil, S. Owen, A. Miklius, and M. Lisowski (2002a), The 12 September 1999 upper east rift zone dike intrusion at Kilauea volcano, Hawaii, *J. Geophys. Res.*, *107*(B7), 2150, doi:10.1029/2001JB000602.

Cervelli, P., P. Segall, K. Johnson, M. Lisowski, and A. Miklius (2002b), Sudden aseismic fault slip on the south flank of Kilauea volcano, *Nature*, *415*(6875), 1014–1018.

Choi, K., A. Bilich, K. Larson, and P. Axelrad (2004), Modified sidereal filtering: Implications for high-rate GPS positioning, *Geophys. Res. Lett.*, *31*(22), L22608, doi:10.1029/2004GL021621.

Dzurisin, D. (2007), *Volcano Deformation: Geodetic Monitoring Techniques*, Springer-Verlag, Berlin.

Elósegui, P., J. Davis, J. Johansson, and I. Shapiro (1996), Detection of transient motions with the Global Positioning System, *J. Geophys. Res.*, *101*(B5), 11249–11261.

Foster, J., and M. Bevis (2003), Lognormal distribution of precipitable water in Hawaii, *Geochem. Geophys. Geosyst.*, *4*(7), 1065, doi:10.1029/2002GC000478.

Foster, J., M. Bevis, Y.-L. Chen, S. Businger, and Y. Zhang (2003), The Ka'u storm (November 2000): Imaging precipitable water using GPS, *J. Geophys. Res.*, *108*(D18), 4585, doi:10.1029/2003JD003413.

Genrich, J., and Y. Bock (1992), Rapid resolution of crustal motion at short ranges with the global positioning system, *J. Geophys. Res.*, *97*(B3), 3261–3269.

Georgiadou, Y., and A. Kleusberg (1988), On carrier signal multipath effects in relative GPS positioning, *Manuscr. Geod.*, *13*, 172–179.

Heliker, C., and T. N. Mattox (2003), The first two decades of the Pu'u 'Ō'ō-Kupaianaha eruption: Chronology and selected bibliography, in *The Pu'u 'Ō'ō-Kupaianaha Eruption of Kilauea Volcano, Hawaii: The First 20 Years*, edited by C. Heliker et al., *U.S. Geol. Surv. Prof. Pap. 1676*, 1–27.

Irwan, M., F. Kinata, N. Fujii, S. Nakao, H. Watanabe, M. Ukawa, E. Fujita and K. Kawai (2003), Rapid crustal deformation caused by magma migration in the Miyakejima Volcano, Japan, *Earth, Planets, Space*, *54*, e13–e16.

Ji, C., K. M. Larson, Y. Tan, K. W. Hudnut, and K. Choi (2004), Slip history of the 2003 San Simeon earthquake constrained by combining 1-Hz GPS, strong motion, and teleseismic data, *Geophys. Res. Lett.*, *31*, L17608, doi:10.1029/2004GL020448.

Jónsson, S., H. Zebker, P. Cervelli, P. Segall, H. Garbeil, P. Mouginis-Mark, and S. Rowland (1999), A shallow-dipping dike fed the 1995 flank eruption at Fernandina volcano, Galpagos, observed by satellite radar interferometry, *J. Geophys. Res.*, *26*(8), 1077–1080.

Langbein, J., and Y. Bock (2004), High-rate real-time GPS network at Parkfield: Utility for detecting fault slip and seismic displacements, *Geophys. Res. Lett.*, *31*, L15S20, doi:10.1029/2003GL019408.

Langbein, J., J. R. Murray, and H. A. Snyder (2006), Coseismic and initial postseismic deformation from the 2004 Parkfield, California earthquake, observed by global positioning system, electronic distance meter, creepmeters, and borehole strainmeters, *Bull. Seis. Soc. Am.*, *96*, doi:10.1785/0120050823, S304–S320.

Larson, K. M. (2009), GPS Seismology, *J. Geodesy*, *83*(3), 227–233, doi:10.1007/s00190-008-0233-x.

Larson, K., A. Bilich, and P. Axelrad (2007), Improving the precision of high-rate GPS, *J. Geophys. Res.*, *112*, B05422, doi:10.1029/2006JB004367.

Larson, K., P. Bodin, and J. Gomberg (2003), Using 1 Hz GPS data to measure deformations caused by the Denali fault earthquake, *Science*, *300*, 1421–1424, doi:10.1126/science.1084531.

Larson, K., P. Cervelli, M. Lisowski, A. Miklius, P. Segall, and S. Owen (2001), Volcano monitoring using GPS. I. Filtering strategies, *J. Geophys. Res.*, *106*(B9), 19,453–19,464, doi:10.1029/2001JB000305.

Larson, K. M., E. E. Small, E. Gutmann, A. Bilich, J. Braun, and V. Zavorotny (2008), Use of GPS receivers as a soil moisture network

for water cycle studies, *Geophys. Res. Lett.*, *35*, L24405, doi:10.1029/2008GL036013.

Larson, K. M., F. H. Webb, and D. C. Agnew (1991), Application of the global positioning system to crustal deformation measurements. II. The influence of orbit determination networks, *J. Geophys. Res.*, *96*(B10), 16,567–16,584.

Lichten, S. and J. Border (1987), Strategies for high-precision global positioning system orbit determination, *J. Geophys. Res.*, *92*(B12), 12,751–12,762.

Lisowski, M., D. Dzurisin, R. P. Denlinger, and E. Y. Iwatsubo (2008), Analysis of GPS-measured deformation associated with the 2004–2006 dome-building eruption of Mount St. Helens, Washington, in *A Volcano Rekindled: The Renewed Eruption of Mount St. Helens*, 2004–2006, *U.S. Geol. Surv. Prof. Pap. 1750*, 301–333.

Lu, Z., C. Wicks, D. Dzurisin, W. Thatcher, J. Freymueller, S. McNutt, and D. Mann (2000), Aseismic inflation of Westdahl volcano, Alaska, revealed by satellite radar interferometry, *Geophys. Res. Lett.*, *27*(11), 1567–1570.

Mattia, M., M. Palano, M. Aloisi, V. Bruno, and Y. Bock (2008), High-rate GPS data on active volcanoes: An application to the 2005–2006 Mt. Augustine (Alaska, USA) eruption, *Terra Nova*, *20*(2), 134–140, doi:10.1111/j.1365–3121.2008.00798.x.

Mattia, M., M. Rossi, F. Guglielmino, M. Aloisi, and Y. Bock (2004), The shallow plumbing system of Stromboli Island as imaged from 1 Hz instantaneous GPS positions, *Geophys. Res. Lett.*, *31*, L24610, doi:10.1029/2004GL021281.

Miyazaki, S., T. Iwabuchi, K. Heki, and I. Naito (2003), An impact of estimating tropospheric delay gradients on precise positioning in the summer using the Japanese nationwide GPS array, *J. Geophys. Res.*, *108*(B7), 2335, doi:10.1029/2000JB000113.

Montgomery-Brown, E. K., D. Sinnett, M. P. Poland, P. Segall, T. Orr, T. H. Zebker, and A. Miklius (2010), Geodetic evidence for en echelon dike emplacement and concurrent slow-slip during the June 2007 intrusion and eruption at Kīlauea volcano, Hawaii, *J. Geophys. Res.*, doi:10.1029/2009JB006658, in press.

Niell, A. E. (1996), Global mapping functions for the atmosphere delay at radio wavelengths, *J. Geophys. Res.*, *101*(B2), 3227–3246, doi:10.1029/95JB03048.

Owen, S., P. Segall, M. Lisowski, M. Murray, M. Bevis, and J. Foster (2000), The January 30, 1997 eruptive event on Kilauea Volcano, Hawaii, as monitored by continuous GPS, *Geophys. Res. Lett.*, *27*(17), 2757–2560.

Patanè, D., M. Mattia, G. Di Grazia, F Cannavò, E. Giampiccolo, C. Musumeci, P. Montalto, and E. Boschi (2007), Insights into the dynamic processes of the 2007 Stromboli eruption and possible meteorological influences on the magmatic system, *Geophys. Res. Lett.*, *34*, L22309, doi:10.1029/2007GL031730.

Poland, M., A. Miklius, T. Orr, J. Sutton, C. Thornber, and D. Wilson (2008), New episodes of volcanism at Kilauea volcano, Hawaii, *Eos Trans. AGU*, *89*(5), 37–38, doi:10.1029/2008EO050001.

Pritchard, M. E., and M. Simons (2004), An InSAR-based survey of volcanic deformation in the southern Andes, *Geophys. Res. Lett.*, *31*, L15610, doi:10.1029/2004GL020545.

Segall, P., P. Cervelli, S. Owen, M. Lisowski, and A. Miklius (2001), Constraints on dike propagation from continuous GPS measurements, *J. Geophys. Res.*, *106*(B9), 19301–19318.

Segall, P., E. K. Desmarais, D. Shelly, A. Miklius, and P. Cervelli (2006), Earthquakes triggered by silent slip events on Kilauea volcano, Hawaii, *Nature*, *442*(7098), 71–74.

Wicks, C. W., Jr., D. Dzurisin, S. Ingebritsen, W. Thatcher, Z. Lu, and J. Iverson (2002), Magmatic activity beneath the quiescent Three Sisters volcanic center, central Oregon Cascade Range, USA, *Geophys. Res. Lett.*, *29*(7), 1122, doi:10.1029/2001GL014205.

Zumberge, J. F., M. B. Heflin, D. C. Jefferson, M. M. Watkins, and F. H. Webb (1997), Precise point positioning for the efficient and robust analysis of GPS data from large networks, *J. Geophys. Res.*, *102*(B3), 5005–5018, doi:10.1029/96JB03860.

K. M. Larson, Department of Aerospace Engineering Sciences, University of Colorado, Boulder, CO 80309-0429, USA. (kristinem.larson@gmail.com)

A. Miklius and M. Poland, U.S.G.S. Hawaiian Volcano Observatory, Hawai'i Volcanoes National Park, P.O. Box 52, Hawai'i National Park, HI 96718, USA. (asta@usgs.gov)